Taylor & Francis
Taylor & Francis Group

Influence of the Temperature and 2,5-Dimethylfuran Concentration on Its Sooting Tendency

Katiuska Alexandrino, Pablo Salvo, Ángela Millera, Rafael Bilbao, and María U. Alzueta

Department of Chemical and Environmental Engineering, Aragón Institute of Engineering Research (I3A), University of Zaragoza, Zaragoza, Spain

ABSTRACT

The sooting tendency of 2,5-dimethylfuran (2,5-DMF), as a proposed fuel or fuel additive, has been studied in a flow reactor at different reaction temperatures (975, 1075, 1175, 1275, 1375, and 1475 K) and inlet 2,5-DMF concentrations (5000, 7500, and 15,000 ppm) under pyrolytic conditions. The quantification of soot and light gases has been done. Additionally, the experimental results of the light gases have been simulated with a detailed gas-phase chemical kinetic model. The experimental results indicate that the temperature has a great influence on both the soot and gas yields, as well as on the concentration of the light gases of pyrolysis. The inlet 2,5-DMF concentration influences the soot yield, whereas no significant effect is observed on the gas yield.

Introduction

Diesel engines have been recognized as one of the most significant sources of soot and are subjected to strict regulations. In diesel engines, the fuel and air typically do not mix as completely as they do in gasoline engines. The non-perfect mixing between the fuel and air may create locally fuel-rich areas where soot is produced when the fuel is ignited.

The reduction of diesel engine soot emissions can be achieved through at least three different strategies: engine modification, exhaust after-treatment, and fuel reformulation. Fuel reformulation usually includes the addition of oxygenated compounds to fuel. Oxygenates contain hydrocarbon functional groups, thus they can also form soot precursors (Barrientos et al., 2013). However, the oxygen present in the oxygenated additives favors the oxidation processes, thereby reducing emissions of soot. The reduction of soot emissions from a diesel engine using oxygenated fuel additives has been confirmed in both experimental (Cheung et al., 2011; Wang et al., 2009) and numerical (Westbrook et al., 2006) studies. However, it is known that, among other factors, the sooting tendency depends strongly on the structure of the oxygenated compound (Barrientos et al., 2013; Esarte et al., 2010; Ladommatos et al., 1996; McEnally and Pfefferle, 2011). For example, the sooting tendency of aliphatic and aromatic compounds is different, mainly because of the different routes involved in the formation of soot. While aliphatics appear to first form acetylene and polyacetylenes, which is a slow process, aromatics can form soot both by

this route and also by a more direct pathway involving ring condensation or polymerization reactions building on the existing aromatic structure (Graham et al., 1975).

2,5-Dimethylfuran (C_6H_8O, 2,5-DMF) is an oxygenated aromatic compound that was originally proposed for its use as biofuel in spark-ignition gasoline (SI) engines (Daniel et al., 2011; Zhong et al., 2010;) because it seems to be better in terms of transportation and storage than ethanol (Binder and Raines, 2009; Roman-Leshkov et al., 2007), which is the main oxygenate used nowadays in reformulated gasolines. The investigation on 2,5-DMF has been recently expanded to be used in compression-ignition (CI) engines (Chen et al., 2013; Liu et al., 2013; Zhang et al., 2013), showing that 2,5-DMF can also be used in these engines. However, the question is if 2,5-DMF, an aromatic, would be a good candidate to be used as a fuel additive aiming to reduce soot emissions from diesel engines.

In a previous work (Alexandrino et al., 2015) on the pyrolysis and oxidation of 2,5-DMF, we quantify the soot amount formed in one selected experiment of pyrolysis of 6000 ppm of 2,5-DMF in a flow reactor setup at the temperature of 1475 K. The results revealed that 2,5-DMF is capable of producing large soot amounts. For this reason, and with the aim of addressing the sooting tendency of 2,5-DMF, we decided to extend the investigation studying the influence of the reaction temperature and the inlet 2,5-DMF concentration on the soot formation during the 2,5-DMF pyrolysis.

It is well known that polycyclic aromatic hydrocarbons (PAH), organic substances containing two or more fused aromatic rings, some of which are classified as carcinogenic and mutagenic, are closely related to soot because they have an important role in soot formation and can remain adsorbed on the soot surface (Sánchez et al., 2013). For this reason, some researchers have evaluated the sooting tendency of 2,5-DMF considering both the PAH and its main precursors amounts formed in the 2,5-DMF conversion. Djokic et al. (2013) studied the thermal decomposition of 2,5-DMF in a bench-scale pyrolysis setup and they detected a high tendency of 2,5-DMF to form large PAH amounts, even under diluted conditions. Aromatics, such as benzene and toluene, were products obtained at high 2,5-DMF conversion. A high fraction of 2,5-DMF was also converted to 1,3-cyclopentadiene, which is known to play a significant role in the formation of PAH and soot (Kim et al., 2010). Cheng et al. (2014) studied the 2,5-DMF pyrolysis in a flow reactor at various pressures (30, 150, and 760 Torr). They compared the results of the 2,5-DMF pyrolysis and of C_6–C_7 cycloalkene pyrolysis, specifically cyclohexane and methylcyclohexane, under very close conditions and observed that the levels of aromatics in the 2,5-DMF pyrolysis are more elevated, which implies the potentially high sooting tendency of 2,5-DMF. Through their gas-phase detailed pyrolysis model of 2,5-DMF, the authors observed that the cyclopentadienyl radical (C_5H_5), the phenyl radical (C_6H_5), and benzene are the most important precursors of large PAH in the pyrolysis of 2,5-DMF. Togbé et al. (2014), in their work of 2,5-DMF performed under premixed low-pressure flame conditions, compared the results with those obtained in flames studies of other compounds: furan, 2-methylfuran, *n*-butane, 1-butene, cyclohexane, dimethylether, ethanol, 1-butanol, and methyl propanoate. The highest mole fractions of 1,3-cyclopentadiene and benzene were detected in the 2,5-DMF flame, while the lowest mole fractions of these soot precursors were observed in the ethanol and 1-butanol flames. Tran et al. (2015) performed simulations for flames of 2,5-DMF and gasoline surrogate (13.7% *n*-heptane, 42.9% iso-octane, 43.4% toluene, in volume), *n*-heptane, iso-octane, and toluene. The results show that only pure toluene leads to higher PAH mole fractions than 2,5-DMF.

In this context, the present study analyzes the formation of soot and gas products in the 2,5-DMF pyrolysis performed in a flow reactor installation under well-controlled experimental conditions, in the temperature and inlet 2,5-DMF concentration intervals of 975–1475 K and 5000–15,000 ppm, respectively. Also, in order to get a better understanding of the different gas-phase processes involved in the 2,5-DMF pyrolysis, experimental results of the gases have been compared with numerical calculations from a detailed gas-phase kinetic mechanism used with success in our earlier publication on the pyrolysis and oxidation of 2,5-DMF (Alexandrino et al., 2015), which includes the reaction sub-mechanism for 2,5-DMF and some intermediate products by Sirjean et al. (2013) and the mechanism progressively developed by our group for hydrocarbon conversion (Abián et al., 2011; Alzueta et al., 2013; Dagaut et al., 2008; Glarborg et al., 1998).

Experimental section

The 2,5-DMF pyrolysis experiments are carried out at different temperatures (975, 1075, 1175, 1275, 1375, and 1475 K) and inlet 2,5-DMF concentrations (5000, 7500, and 15,000 ppm). Experiments are conducted in a N_2 atmosphere using a facility suitable for the soot formation and collection. The experimental setup consists of four systems: the gas feed system, the reaction system, the soot collection system, and the gas analysis system. This experimental setup has been used with success in a number of different studies related to soot formation (Abián et al., 2014; Esarte et al., 2010; Ruiz et al., 2007a; Sánchez et al., 2013).

The pyrolysis takes place in a quartz flow reactor (Figure 1), which is placed vertically in an electrically heated furnace. The reactor consists of three parts, namely: (a) the head, which has two entries where the gases are fed; (b) the body with an internal diameter of 45 mm and length of 800 mm; and (c) the mobile probe, which allows controlling the reaction volume. The reactor inlet and outlet are cooled by an air flow, and the temperature profile inside the reactor is determined at nonreacting conditions by means of an S-type thermocouple. Thus, the gases are mixed to the reactor inlet and then flow through an isothermal section so-called "reaction zone," which is considered to be around 16 cm in length.

Accordingly, 2,5-DMF gas is fed into the reactor by a single inlet, by means of 2,5-DMF liquid pumped by an isocratic HPLC pump, which passes through a thermally isolated line using N_2 as the carrier gas. The total gas flow rate is 1000 mL(STP)/min, which corresponds to a residence time as function of temperature of 4168/T(K). N_2 is used to close the balance, and this flow is introduced to the reactor by the second individual inlet. The N_2 flows are controlled through mass flow controllers. A pressure transducer located at the inlet of the reactor ensures that a constant pressure is maintained in the reactor. Experiments are generally run for 3 h, not exceeding an overpressure limit of 1.3 bar inside the reactor in order to avoid perturbations in the experimental setup.

The reactor outlet is linked to the soot collection system. This system consists of a quartz fiber filter, with a pore diameter lower than 1 μm, in which soot is collected. Furthermore, the soot remaining on the reactor walls is also recovered when the experiment ends. The total soot amount is determined as the sum of the soot collected both in the filter and in the reactor walls.
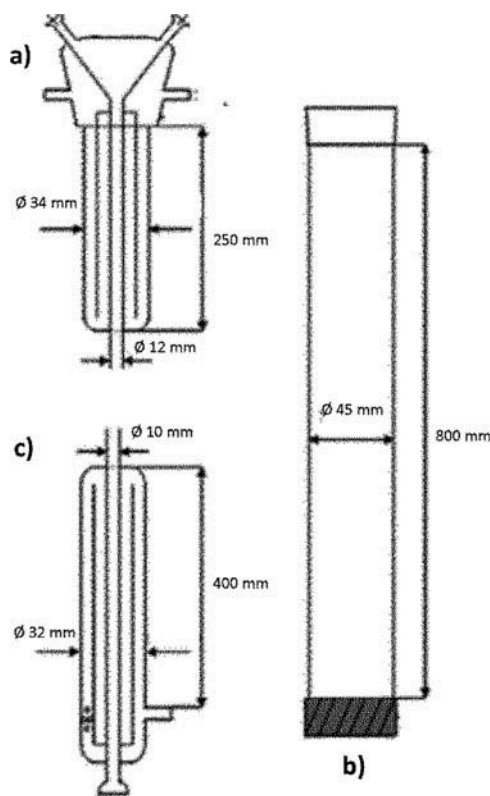
Figure 1. Reactor scheme.

The gas product stream, after leaving the reactor and the soot collection system, passes across a filter to retain solid particles that may remain in the gas and are then analyzed using an Agilent 6890 gas chromatograph equipped with a thermal conductivity detector (TCD) and a flame ionization detector (FID). This analysis equipment provides an 130 accuracy of ±10 ppm and is calibrated with 2,5-DMF, 2-methylfuran (2-MF), and a patron mixture of C_2H_2, C_2H_5OH, CO, CO_2, H_2, CH_4, C_2H_4, C_2H_6, propane, propylene, propadiene, 1,3-butadiene, isobutane, n-butane, C_6H_6, C_7H_8, and xylene.

Results

The main aim of this work has been to carry out an experimental study of the sooting 135 tendency of 2,5-DMF from its pyrolysis by varying the principal operating conditions, such as reaction temperature (from 975 to 1475 K in intervals of 100 K) and inlet 2,5-DMF concentration (5000, 7500, and 15,000 ppm) under well-controlled experimental conditions.

Additionally, to provide a support for a better understanding of the different gas-phase processes involved in the 2,5-DMF pyrolysis, the experimental results of the main product gases 140 quantified have been simulated in terms of a detailed gas-phase chemical kinetic model for the 2,5-DMF pyrolysis and oxidation mentioned before (Alexandrino et al., 2015), using the Senkin code in conjunction with the CHEMKIN-II library (Kee et al., 1991). The model does not

include soot formation processes, and only includes a reaction sub-mechanism reacting up to naphthalene (Sirjean et al., 2013). Thus, the purpose is to analyze the yield profiles trends of the main gaseous products quantified and not to reproduce exactly the experimental data.

Figure 2 shows the experimental and model calculations of the 2,5-DMF conversion for each reaction temperature and inlet 2,5-DMF concentration studied. Model calculations cover a wider range of temperature, and through the results it is observed that 2,5-DMF starts to be converted around 900 K. The 2,5-DMF conversion is 100%, or nearly 100%, for temperatures above 1175 K. However, at 1075 K the experimental 2,5-DMF conversion is between 77% and 95%, depending on its inlet concentration.

According to modeling calculations, the main channel for 2,5-DMF consumption under pyrolytic conditions appears to be the abstraction of hydrogen from the methyl group to yield the resonance-stabilized 5-methyl-2-furanylmethyl radical. Subsequent reactions, which include as intermediates phenol (C_6H_5OH), phenoxy radicals (C_6H_5O), and a bicycle, result in the formation of the cyclopentadienyl radical (C_5H_5). The overall reaction (R1), as a possible pathway to give the cyclopentadienyl radical, has also been confirmed in the works of Olivella et al. (1995) and D'Anna (2005):

$$C_6H_5O \rightarrow C_5H_5 + CO \qquad (R1)$$

The importance of cyclopentadienyl as a precursor radical in the growth process to larger and larger PAH, without passing through benzene as an intermediate, has already been investigated. In this way, the odd-carbon-atom pathway of the cyclopentadienyl radical dimerization to form naphthalene [reaction (R2)], has been proposed in the literature (e.g., Castaldi et al., 1996; Marinov et al., 1996):
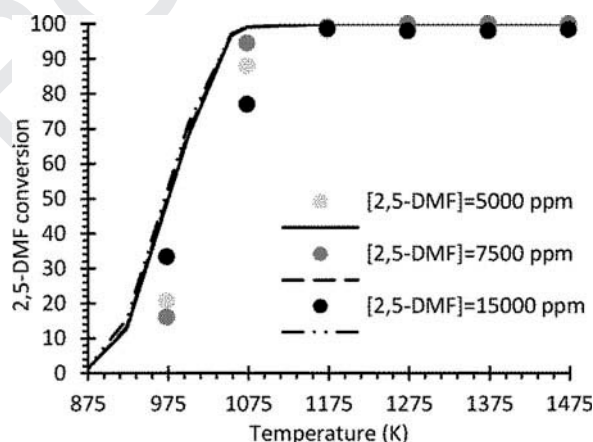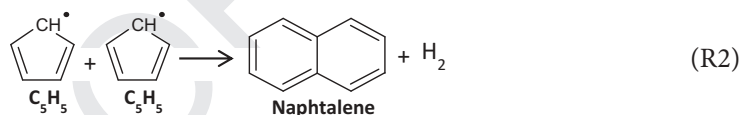
(R2)

Figure 2. Experimental (points) and calculated (lines) 2,5-DMF conversion, as a function of temperature, and for different inlet 2,5-DMF concentrations.
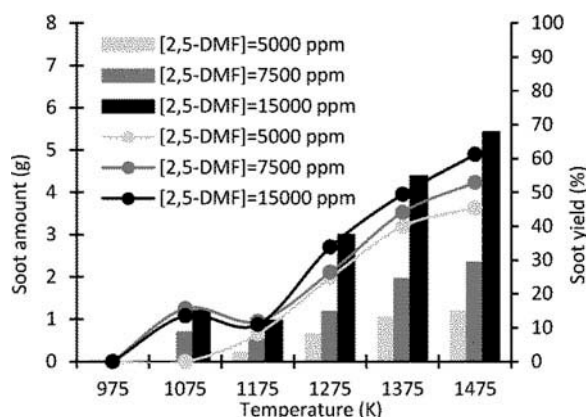
Figure 3. Soot amount (bars) and soot yield (lines with points) found in the 2,5-DMF pyrolysis, in the 975–1475 K temperature range, and for different inlet 2,5-DMF concentration.

Figure 3 reports the total soot amount collected (in g) and the soot yield (in %), in all of the experiments. The soot yield is defined as the percentage of the carbon amount in soot related to the carbon amount fed into the reactor (Esarte et al., 2009). In Figure 3, it is observed that for any inlet 2,5-DMF concentration no soot formation occurs at 975 K. For a fixed temperature, an increase in the inlet 2,5-DMF concentration leads to an increase 170 both in the soot amount and in the soot yield, with a more significant influence of the inlet 2,5-DMF concentration at high temperatures, as it has been already reported earlier for other hydrocarbons and oxygenated compounds (Esarte et al. 2009; Ruiz et al., 2007a; Sánchez et al., 2013).

For a fixed 2,5-DMF concentration, the expected trend is that the soot amount formed 175 increases with the increase of the temperature. This trend happens for the concentration of 5000 ppm of 2,5-DMF throughout the temperature range studied. However, for the concentrations of 7500 and 15,000 ppm of 2,5-DMF, this trend occurs in the 1175–1475 K temperature range. For these two concentrations, at 1075 K both the soot amount and the soot yield are slightly greater than at 1175 K. As mentioned in the experimental section, 180 the soot amount shown in Figure 3 is the sum of the soot collected from both the filter and the reactor walls. No soot was found on the reactor walls at 1075 K; however, there was soot on the reactor walls at 1175 K. Besides, the weight of the filter where soot was collected was slightly greater at 1075 K than at 1175 K. This is because at these two temperatures, and for 7500 and 15,000 ppm of 2,5-DMF, the formation of a condensate 185 occurs, which is higher, according to the results obtained, at 1075 K. Due to the difficulty in quantifying soot at low temperatures (1075 and 1175 K), because of the formation of the condensate, the soot amount values for 7500 and 15,000 ppm of 2,5-DMF shown in Figure 3 should be considered with caution. Also, it is worth mentioning that with 15,000 ppm of 2,5-DMF and at 1175 K, when 2.5 h of experiment had elapsed, the pressure inside 190 the reactor went up to the overpressure limit (1.3 bar), and the experiment was stopped. This rise in pressure was attributed to the deposit of thin particles of soot and condensate in the filters. However, since the experiments are performed under steady state conditions, the values of soot amount and yield presented for this experiment in Figure 2 are extrapolated to 3 h.   195

In order to get some insight on the condensate formed, a qualitative analysis was carried out with the sample obtained from the experiment of 15,000 ppm of 2,5-DMF at 1075 K using a 7890A gas chromatograph coupled to a mass spectrometer 5975C mass selective detector of Agilent Technologies (Sánchez et al., 2013). The species detected are summarized in Table 1, together with their molecular structures and boiling points at 200 atmospheric pressure. In general, the species found in the condensate are volatile PAH.

Because acetylene is regarded as one of the main soot precursors via the HACA (hydrogen abstraction–C_2H_2 addition) mechanism (Appel et al., 2000; Frenklach, 2002), it would be interesting to compare the soot yields obtained in the C_2H_2 pyrolysis (Ruiz et al., 2007b) with those obtained in the present work from the 2,5-DMF pyrolysis. 205 Figure 4 shows the soot yield found in the pyrolysis of 30,000 ppm of total carbon ($[C_2H_2]$ = 15,000 ppm and $[C_6H_8O]$ = 5000 ppm) for 1275, 1375, and 1475 K. It is noticeable that the soot yield for 2,5-DMF is very close to the soot yield for acetylene. This high-sooting tendency of 2,5-DMF could be attributed to the formation of cyclopentadienyl radicals during the 2,5-DMF pyrolysis, which favors the formation of PAH and 210 consequently the soot formation, as mentioned above.
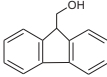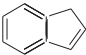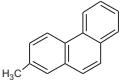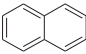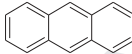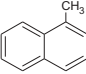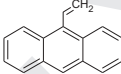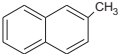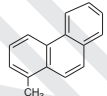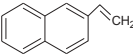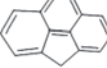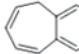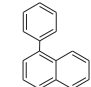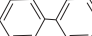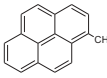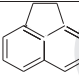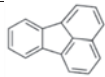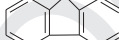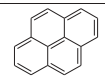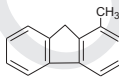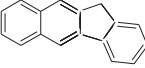
Apart from the formation of soot, unreacted 2,5-DMF and different light gases produced, such as: ethane (C_2H_6), 1,3-butadiene (C_4H_6), toluene ($C_6H_5CH_3$), ethylbenzene ($C_6H_5C_2H_5$), propadiene (C_3H_4), 2-methylfuran (C_5H_6O), ethylene (C_2H_4), acetylene (C_2H_2), hydrogen (H_2), benzene (C_6H_6), methane (CH_4), carbon monoxide (CO), and 215 carbon dioxide (CO_2), have been identified and quantified. These last seven compounds were the major gas products found in all of the experiments. The other gases were found only at 975 and 1075 K, and some of them were also found at 1175 K in small quantities (toluene and ethylbenzene). The quantification of the principal gases allows to analyze the 2,5-DMF conversion processes and further findings related to soot production. 220

Figure 5 shows the gas yield (in %) as a function of temperature for the different inlet 2,5-DMF concentrations studied. The gas yield is defined as the percentage of the carbon amount in outlet gases related to the carbon amount fed into the reactor (Esarte et al., 2009). It is worth clarifying that the gas yield includes the 2,5-DMF amount found at the reactor outlet. As can be see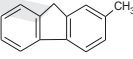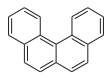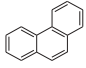n, for the different inlet 2,5-DMF concentrations, increasing 225 temperature causes the gas yield to decrease. Regarding the influence of the inlet 2,5-DMF concentration, it does not present a clear trend as a function of temperature. The sum of the soot and gas yields, Figures 3 and 5 respectively, is not 100% because other by-products, such as PAH and pyrolytic carbon, are formed and not are quantified here.

The yield to the major gas products found for different temperatures and inlet 2,5-DMF 230 concentrations is shown in Figures 6–10, as symbols and lines for experimental and modeling data, respectively. For each carbonaceous product (2-MF, C_2H_4, C_2H_2, C_6H_6, CH_4, CO, and CO_2), the yield is defined as the percentage of the carbon moles of the gas produced in the experiment, related to the carbon moles fed into the reactor. On the other hand, the H_2 yield is defined as the percentage of H moles present in H_2, related to the H 235 moles fed into the reactor.

The 2-methylfuran (2-MF) yield, an important intermediate from the pyrolysis and oxidation of 2,5-DMF (Sirjean et al., 2013), is represented in Figure 6. From the model predictions it is observed that the yield profile of 2-MF presents a maximum value at approximately 975 K, then it is consumed to form soot precursors. 2-MF is completely 240 consumed from 1175 K.

Table 1. Species with their molecular structures and boiling points (BP at 760 mmHg) found in the condensate formed at low temperature, for [2,5-DMF] = 15,000 ppm and 1075 K.

Species	Molecular structure	BP (K)	Species	Molecular structure	BP (K)
1,3,5,7-Cyclooctatetraene		416	Fluorene-9-methanol		610
Indene		454	2-methyl-Phenanthrene		612
Naphthalene		491	Anthracene		613
1-methyl-Naphthalene		514	9-ethenyl-Anthracene		334–339 (10 mmHg)
2-methyl-Naphthalene		516	1-methyl-Phenanthrene		626
2-ethenyl-Naphthalene		408 (18 mmHg)	4H-Cyclopenta[def]phenanthrene		626
Benzocycloheptatriene		521	2-phenyl-Naphthalene		631
Biphenyl		528	1-methyl-Pyrene		645
Acenaphthene		552	Fluoranthene		648
Fluorene		568	Pyrene		666
1-methyl-9H-Fluorene		587	11H-Benzo[b]fluorene		675
2-methyl-9H-Fluorene		591	Benzo[c]phenanthrene		710
Phenanthrene		609	Triphenylene		711

Figures 7a and 7b present the ethylene and acetylene yields, respectively. It is observed that, from 1175 K, the ethylene yield (Figure 7a) decreases with the increase of temperature to give acetylene. Modeling results follow the same trend as the experimental results with higher deviations at 1075 and 1175 K. Regarding the influ- 245 ence of the inlet 2,5-DMF concentration, it is observed that, from the experimental
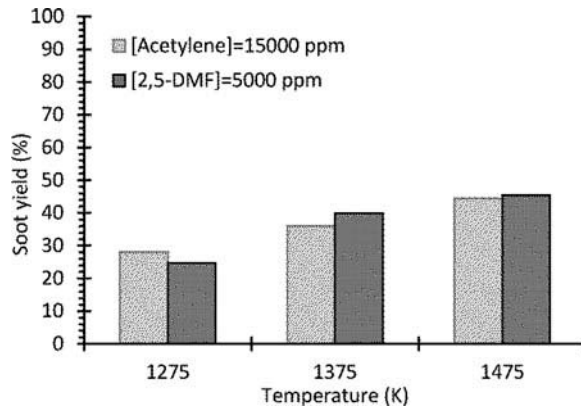
Figure 4. Comparison of the soot yield obtained in the acetylene pyrolysis with that obtained in the 2,5-DMF pyrolysis, as a function of temperature, under the same operational conditions: $Q_{Total} = 1000$ mLN/min, [Carbon] = 30,000 ppm.
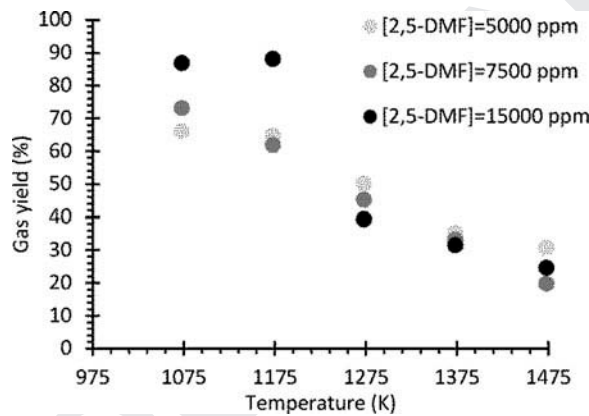
Figure 5. Gas yield from the 2,5-DMF pyrolysis in the 975–1475 K temperature range.

results, the highest ethylene yield corresponds to the lowest inlet 2,5-DMF concentration. Figure 7b indicates that the experimental acetylene yield exhibits a maximum at 1275 K, being acetylene consumed above this temperature. The trend of the model predictions is in good agreement with the experimental results up to 1275 K, but no 250 maximum is predicted. This disagreement between both experimental and modeling trends above 1275 K is probably due to the participation of C_2H_2 in the aromatic growth to lead to the formation of PAH through the HACA mechanism, which involves the growth of large aromatic structures through sequential hydrogen abstraction and acetylene addition (Frenklach et al., 1985). Above this temperature, the model 255 does not fit the experimental data trend because, as it has been mentioned, the model does not account for the formation of PAH or soot. Regarding the influence of the inlet 2,5-DMF concentration, the lower the inlet 2,5-DMF concentration, the higher the acetylene yield in the outlet stream.

Figure 6. Experimental (symbols) and calculated (lines) 2-MF (C_5H_6O) yield from the pyrolysis of 5000, 7500, and 15,000 ppm of 2,5-DMF, in the 975–1475 K temperature range.
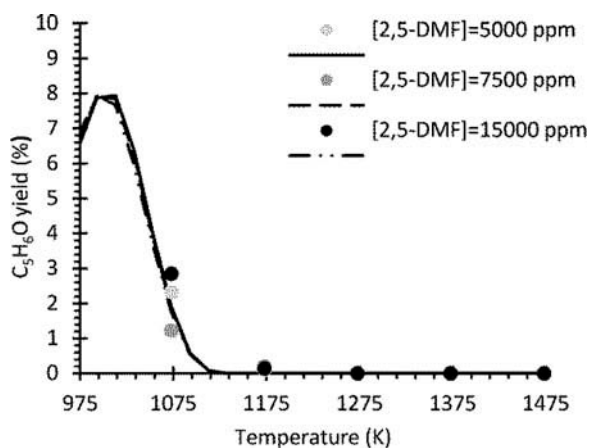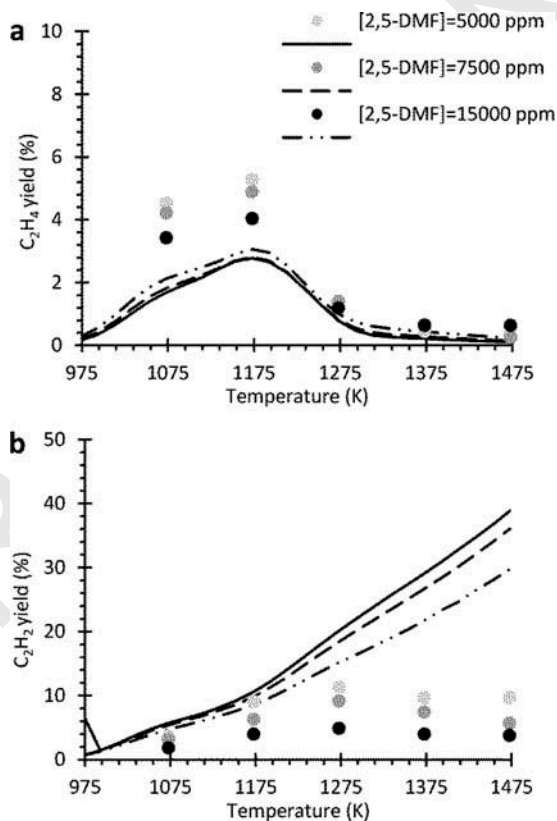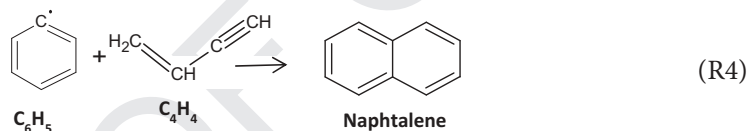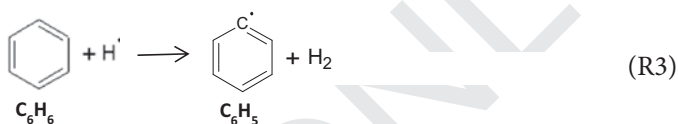

Figure 7. Experimental (symbols) and calculated (lines) C_2H_4 and C_2H_2 yields from the pyrolysis of 5000, 7500, and 15,000 ppm of 2,5-DMF, in the 975–1475 K temperature range.

Hydrogen, a principal species in the HACA mechanism, and benzene, a key compound 260
in the soot formation process, have been detected and quantified. The yields to these
compounds can be seen in Figures 8a and 8b, respectively. Hydrogen was the main gas
product found in the outlet stream and, as expected, an increase in hydrogen concentra-
tion is observed when the temperature is increased (Figure 8a). Analyzing together the
results for H_2 (Figure 8a) with the soot amount (Figure 3) and the results for acetylene 265
(Figure 7b), the acetylene consumption and hydrogen release, which match with the soot
tendency found in Figure 3, support the hypothesis of soot formation via the growth of
PAH through the HACA mechanism, which is favored at higher temperatures. It is worth
mentioning that for hydrogen the model follows the same trend as the experimental
results, fitting well to the results up to 1175 K. However, at 1275 K and above, the 270
model underestimates the experimental results. This fact can be due, once more, to the
non-inclusion of soot formation reactions; thus, the model is not accounting for the
hydrogen release associated to large PAH formation. Also, it is seen that for the lowest

$$\text{C}_6\text{H}_6 + \text{H}^{\cdot} \longrightarrow \text{C}_6\text{H}_5 + \text{H}_2 \tag{R3}$$

$$\text{C}_6\text{H}_5 + \text{C}_4\text{H}_4 \longrightarrow \text{Naphtalene} \tag{R4}$$

2,5-DMF amount in the reactor inlet, the hydrogen yield decreases. This fact can be
attributed to the reduced soot formation for this inlet 2,5-DMF concentration. 275

The benzene yield, which is a key component in PAH growth reactions since it is
considered the first aromatic ring, reaches a maximum at 1175 K, as can be seen in
Figure 8b. The inlet 2,5-DMF concentration seems to have a slight influence on the
benzene yield. At higher temperatures, the benzene yield decreases because of its con-
sumption to produce larger PAH. According to model calculations, benzene is consumed 280
to give phenyl radical (C_6H_5), which then reacts with vinylacetilene (C_4H_4) to form
naphthalene, through the following reactions:
Figure 9 shows that the presence of methane, a stable gas in the conditions of this work, in
the outlet stream is important, becoming the second carbon compound after CO that was
found in the highest concentration in the gas product stream of all of the experiments. A 285
maximum in the CH_4 yield profile is reached at 1175 K. Its consumption from 1175 K, is
probably implying that methyl radicals, its main precursor, are taking part in reactions
pathways leading to the formation of soot, which formation increases with temperature
(Figure 2). Almost no influence on the methane yields is observed with the inlet 2,5-DMF
concentration. 290

Figure 8. Experimental (symbols) and calculated (lines) H_2 and C_6H_6 yields from the pyrolysis of 5000, 7500, and 15,000 ppm of 2,5-DMF, in the 975–1475 K temperature range.

Figure 9. Experimental (symbols) and calculated (lines) CH_4 yield from the pyrolysis of 5000, 7500, and 15,000 ppm of 2,5-DMF, in the 975–1475 K temperature range.
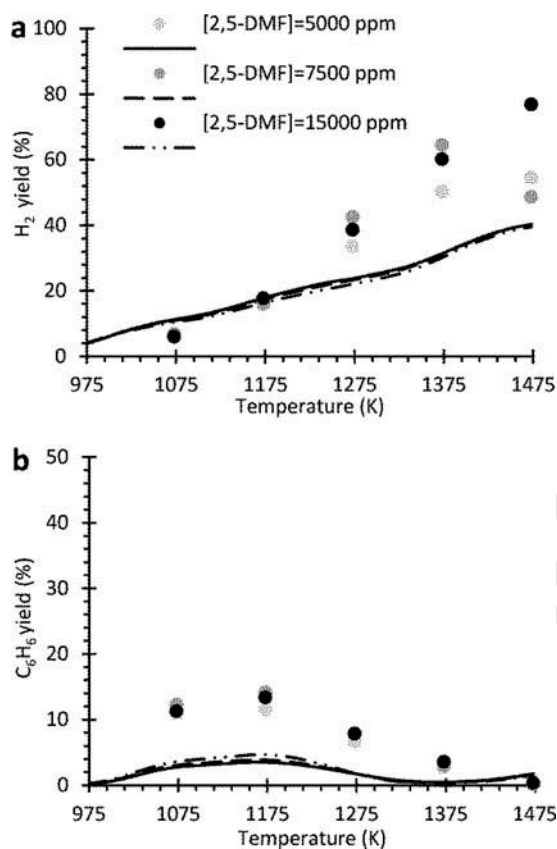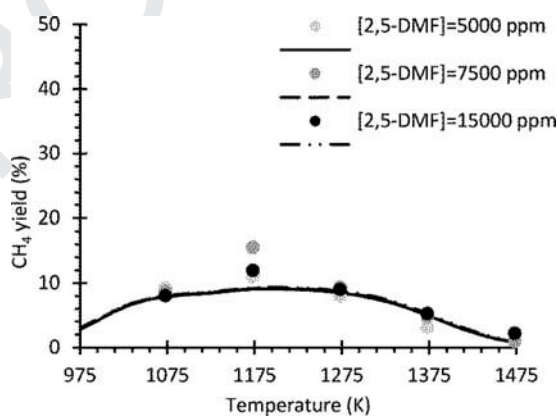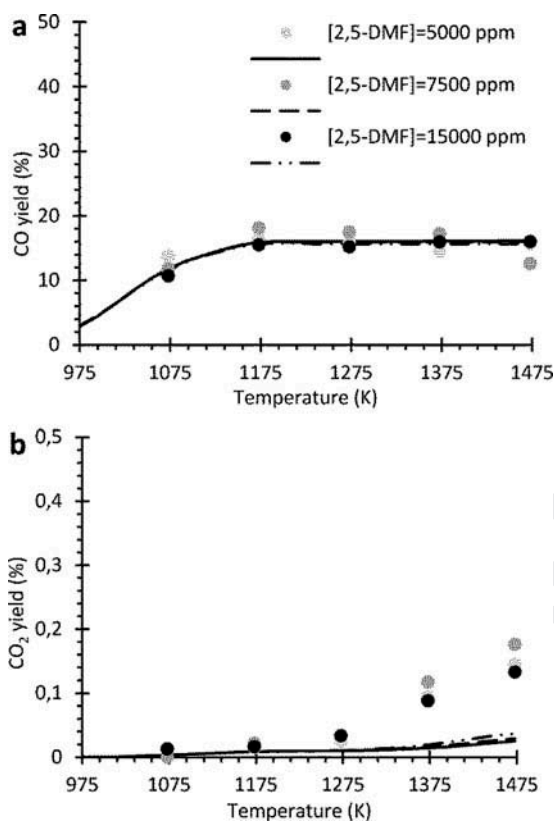
Figure 10. Experimental (symbols) and calculated (lines) CO and CO_2 yields from the pyrolysis of 5000, 7500, and 15,000 ppm of 2,5-DMF, in the 975–1475 K temperature range.

Because oxygenated compounds contain oxygen in their structures, it is expected that amounts of CO and CO_2, perhaps significant, are formed. This fact is important because it means that carbon is removed of the reaction pathways leading to the soot formation, since the oxygen content in 2,5-DMF favors the oxidation of intermediates towards CO and CO_2. Thus, the fraction of carbon remaining in the form of soot precursors decreases. 295 Figures 10a and 10b show the CO and CO_2 yields, respectively.

CO was the major carbon compound found in the experiments. For all of the inlet 2,5-DMF concentrations, the CO yield remains basically constant with increasing temperature from 1175 K. The calculations indicated that the CO main production source at low temperature (1075 K), is the reaction (R1). On the other hand, the CO_2 yield increases 300 monotonically (Figure 10b) as a result of the CO conversion, through the reaction (R5), which is favored at high temperature:

$$CO + OH \rightarrow CO_2 + H \tag{R5}$$

The results obtained in this work, and in the various investigations addressing the formation of soot precursors and soot from 2,5-DMF (Alexandrino et al., 2015; Cheng et al., 2014; Djokic 305 et al., 2013; Kim et al., 2010; Togbé et al., 2014; Tran et al., 2015), suggest that the use of 2,5-DMF as a future fuel or fuel additive, mainly in diesel engines, can be limited due to its high ability to form soot. However, soot emission reduction in diesel engines using 2,5-DMF/diesel mixtures

has shown acceptable results (Chen et al., 2013; Liu et al., 2013; Zhang et al., 2013). Therefore, in order to propose 2,5-DMF as a renewable fuel friendly with the environment, further tests of the 2,5-DMF combustion in engine under specific conditions are needed. 310

Conclusions

This work includes a study on the soot amount and the yield to some light gases formed during the 2,5-DMF pyrolysis in a flow reactor setup at different temperatures (975–1475 K) and inlet 2,5-DMF concentrations (5000, 7500, and 15,000 ppm). A gas- 315 phase detailed kinetic model taken from the literature has been used for simulating the gas-phase experimental data. Since the model does not include reactions related to the soot formation processes (except a reaction sub-mechanism for naphthalene), the fit between the experimental and calculations are not good. However, in general, the model prediction trends are in good agreement with the experimental trends, except 320 for acetylene:

- 2,5-DMF begins to be converted around 900 K, and for temperatures above 1175 K the 2,5-DMF conversion is practically 100%.
- The soot yield is seen to be greater at high temperatures and it is more noticeable with the increase of the inlet 2,5-DMF concentration, reaching yields over 60%. 325 On the other hand, increasing temperature causes the decrease of the gas yield and no significant effect is observed of the inlet 2,5-DMF concentration on the gas yield.
- At 1075 and 1175 K and for the two highest inlet 2,5-DMF concentrations studied (7500 and 15000 ppm), a condensate was formed interfering with the soot quantifi- 330 cation. The condensate was analyzed and, in general, the species found were volatile PAH.
- The oxygen content in 2,5-DMF favors the oxidation of intermediates towards CO and CO_2, and among the gases measured, hydrogen was found in the highest concentration, whereas CO was the major carbon compound found in the 335 experiments.
- 2,5-DMF has a high sooting tendency, which could be explained by their tendency to form cyclopentadienyl radicals, which have importance as precursors in the growth processes to larger and larger PAH, without passing through benzene as intermediate. The ability of 2,5-DMF to form soot is very close to the capacity 340 of acetylene to form soot, which suggests that the use of 2,5-DMF as a future fuel or fuel additive can be limited. In this way, further tests of the 2,5-DMF combustion in engines under specific conditions will determine if 2,5-DMF can be used as an additive.

References

Abián, M., Giménez-López, J., Bilbao, R., and Alzueta, M.U. 2011. Effect of different concentrations levels of CO_2 and H_2O on the oxidation of CO: Experiments and modeling. *Proc. Combust. Inst.*, **33**, 317–323.

Abián, M., Peribáñez, E., Millera, Á., Bilbao, R., and Alzueta, M.U. 2014. Impact of nitrogen oxides (NO, NO_2, N_2O) on the formation of soot. *Combust. Flame*, **161**, 280–287.

Alexandrino, K., Millera, A., Bilbao, R., and Alzueta, M.U. 2015. Novel aspects in the pyrolysis and oxidation of 2,5-dimethylfuran. *Proc. Combust. Inst.*, **25**, 1717–1725.

Alzueta, M.U., Aranda, V., Monge, F., Millera, A., and Bilbao, R. 2013. Oxidation of methyl formate and its interaction with nitric oxide. *Combust. Flame*, **160**, 853–860.

Appel, J., Bockhorn, H., and Frenklach, M. 2000. Kinetic modeling of soot formation with detailed chemistry and physics: laminar premixed flames of C2 hydrocarbons. *Combust. Flame*, **121**, 122–136.

Barrientos, E.J., Lapuerta, M., and Boehman, A.L. 2013. Group additivity in soot formation for the example of C-5 oxygenated hydrocarbon fuels. *Combust. Flame*, **160**, 1484–1498.

Binder, J.B., and Raines, R.T. 2009. Simple chemical transformation of lignocellulosic biomass into furans for fuels and chemicals. *J. Am. Chem. Soc.*, **131**, 1979–1985.

Castaldi, M.J., Marinov, N.M., Melius, C.F., Huang, J., Senkan, S.M., Pitz, W.J., and Westbrook, C. K. 1996. Experimental and modeling investigation of aromatic and polycyclic aromatic hydrocarbon formation in a premixed ethylene flame. *Proc. Int. Symp. Combust.*, **26**, 693–702.

Chen, G., Shen, Y., Zhang, Q., Yao, M., Zheng, Z., and Liu, H. 2013. Experimental study on combustion and emission characteristics of a diesel engine fueled with 2,5-dimethylfuran–diesel, n-butanol–diesel and gasoline–diesel blends. *Energy*, **54**, 333–342.

Cheng, Z., Xing, L., Zeng, M., Dong, W., Zhang, F., Qi, F., and Li, Y. 2014. Experimental and kinetic modeling study of 2,5-dimethylfuran pyrolysis at various pressures. *Combust. Flame*, **161**, 2496–2511.

Cheung, C.S., Zhu, R., and Huang, Z. 2011. Investigation on the gaseous and particulate emissions of a compression ignition engine fueled with diesel–dimethyl carbonate blends. *Sci. Total Environ.*, **409**, 523–552.

Dagaut, P., Glarborg, P., and Alzueta, M.U. 2008. The oxidation of hydrogen cyanide and related chemistry. *Prog. Energy Combust. Sci.*, **34**, 1–46.

Daniel, R., Tian, G., Xu, H., Wyszynski, M. L., Wu, X., and Huang, Z. 2011. Effect of spark timing and load on a DISI engine fueled with 2,5-dimethylfuran. *Fuel*, **90**, 449–458.

D'Anna, A. 2005. Detailed modeling of the molecular growth process in aromatic and aliphatic premixed flames. *Energy Fuels*, **19**, 79–86.

Djokic, M., Carstensen, H., Van Geem, K.M., and Marin, G.B. 2013. The thermal decomposition of 2,5-dimethylfuran. *Proc. Combust. Inst.*, **34**, 251–258.

Esarte, C., Millera, A., Bilbao, R., and Alzueta, M.U. 2009. Gas and soot products in the pyrolysis of acetylene-ethanol blends under flow reactor conditions. *Fuel Process. Technol.*, **90**, 496–503.

Esarte, C., Millera, A., Bilbao, R., and Alzueta, M.U. 2010. Effect of ethanol, dimethylether, and oxygen, when mixed with acetylene, on the formation of soot and gas products. *Ind. Eng. Chem. Res.*, **49**, 6772–6779.

Frenklach, M., Clary, D.W., Gardiner, W.C., and Stein, S.E. 1985. Detailed kinetic modeling of soot formation on shock-tube pyrolysis of acetylene. *Proc. Int. Symp. Combust.*, **20**, 887–901.

Frenklach, M. 2002. Reaction mechanism of soot formation in flames. *Phys. Chem. Chem. Phys.*, **4**, 2028–2037.

Glarborg, P., Alzueta, M.U., Dam-Johansen, K., and Miller, J.A. 1998. Kinetic modeling of hydrocarbon nitric oxide interactions in a flow reactor. *Combust. Flame*, **115**, 1–27.

Graham, S.C., Homer, J.B., and Rosenfeld, J.L.J. 1975. The formation and coagulation of soot aerosols generated by the pyrolysis of aromatic hydrocarbons. *Proc. R. Soc. London, Ser. A*, **344**, 259–285.

Kee, R.J., Rupley, F.M., and Miller, J.A. 1991. Chemkin-II: A Fortran chemical kinetics package for the analysis of gas-phase chemical kinetics. Report SAND87-8215.

Kim, D.H., Mulholland, J.A., Wang, D., and Violi, A. 2010. Pyrolytic hydrocarbon growth from cyclopentadiene. *J. Phys. Chem. A*, **114**, 12411–12416.

Ladommatos, N., Rubenstein, P., and Bennett, P. 1996. Some effects of molecular structure of single hydrocarbons on sooting tendency. *Fuel*, **75**, 114–124.

Liu, H., Xu, J., Zheng, Z., Li, S., and Yao, M. 2013. Effects of fuel properties on combustion and emissions under both conventional and low temperature combustion mode fueling 2,5-dimethyl-furan/diesel blends. *Energy*, **62**, 215–223.

Marinov, N.M., Pitz, W.J., Westbrook, C.K., Castaldi, M.J., and Senkan, S.M. 1996. Modeling of aromatic and polycyclic aromatic hydrocarbon formation in premixed methane and ethane flames. *Combust. Sci. Technol.*, **116–117**, 211–286.

McEnally, C.S., and Pfefferle, L.D. 2011. Sooting tendencies of oxygenated hydrocarbons in laboratory-scale flames. *Environ. Sci. Technol.*, **45**, 2498–2503.

Olivella, S., Solé, A., and García-Raso, A. 1995. Ab initio calculations of the potential surface for the thermal decomposition of the phenoxyl radical. *J. Phys. Chem.*, **99**, 10549–10556.

Roman-Leshkov, R., Barrett, C.J., Liu, Z.Y., and Dumesic, J.A. 2007. Production of dimethylfuran for liquid fuels from biomass-derived carbohydrates. *Nature*, **447**, 982–986.

Ruiz, M.P., Callejas, A., Millera, A., Alzueta, M.U., and Bilbao, R. 2007a. Soot formation from C_2H_2 and C_2H_4 pyrolysis at different temperatures. *J. Anal. Appl. Pyrolysis*, **79**, 244–251.

Ruiz, M.P., Guzmán de Villoria, R., Millera, A., Alzueta, M.U., and Bilbao, R. 2007b. Influence of different operation conditions on soot formation from C_2H_2 pyrolysis. *Ind. Eng. Chem. Res.*, **46**, 7550–7560.

Sánchez, N.E., Millera, Á., Bilbao, R., and Alzueta, M.U. 2013. Polycyclic aromatic hydrocarbons (PAH), soot and light gases formed in the pyrolysis of acetylene at different temperatures: Effect of fuel concentration. *J. Anal. Appl. Pyrolysis*, **103**, 126–133.

Sirjean, B., Fournet, R., Glaude, P., Battin-Leclerc, F., Wang, W., and Oehlschlaeger, M.A. 2013. Shock tube and chemical kinetic modeling study of the oxidation of 2,5-dimethylfuran. *J. Phys. Chem. A*, **117**, 1371–1392.

Togbé, C., Tran, L., Liu, D., Felsmann, D., Oßwald, P., Glaude, P., Sirjean, B., Fournet, R., Battin-Leclerc, F., and Kohse-Höinghaus, K. 2014. Combustion chemistry and flame structure of furan group biofuels using molecular-beam mass spectrometry and gas chromatography—Part III: 2,5-Dimethylfuran. *Combust. Flame*, **161**, 780–797.

Tran, L., Sirjean, B., Glaude, P., Kohse-Hoinghaus, K., and Battin-Leclerc, F. 2015. Influence of substituted furans on the formation of polycyclic aromatic hydrocarbons in flames. *Proc. Combust. Inst.*, **2**, 1735–1743.

Wang, J., Wu, F., Xiao, J., and Shuai, S. 2009. Oxygenated blend design and its effects on reducing diesel particulate emissions. *Fuel*, **88**, 2037–2045.

Westbrook, C.K., Pitz, W.J., and Curran, J.H. 2006. Chemical kinetic modeling study of the effects of oxygenated hydrocarbons on soot emissions from diesel engines. *J. Phys. Chem. A*, **110**, 6912–6922.

Zhang, Q., Chen, G., Zheng, Z., Liu, H., Xu, J., and Yao, M. 2013. Combustion and emissions of 2,5-dimethylfuran addition on a diesel engine with low temperature combustion. *Fuel*, **103**, 730–735.

Zhong, S., Daniel, R., Xu, H., Zhang, J., Turner, D., Wyszynski, M.L., and Richards, P. 2010. Combustion and emissions of 2,5-dimethylfuran in a direct-injection spark-ignition engine. *Energy Fuels*, **24**, 2891–2899.